Available online at www.sciencedirect.com
ScienceDirect
Bioorganic & Medicinal Chemistry Letters
Bioorganic & Medicinal Chemistry Letters 17 (2007) 2886–2889

Synthesis, structural analysis, and SAR studies of triazine derivatives as potent, selective Tie-2 inhibitors

Brian L. Hodous,[a,*] Stephanie D. Geuns-Meyer,[a] Paul E. Hughes,[d] Brian K. Albrecht,[a] Steve Bellon,[c] Sean Caenepeel,[d] Victor J. Cee,[a] Stuart C. Chaffee,[a] Maurice Emery,[e] Jenne Fretland,[e] Paul Gallant,[b] Yan Gu,[b] Rebecca E. Johnson,[a] Joseph L. Kim,[c] Alexander M. Long,[c] Michael Morrison,[b] Philip R. Olivieri,[a] Vinod F. Patel,[a] Anthony Polverino,[d] Paul Rose,[c] Ling Wang[d] and Huilin Zhao[c]

[a]*Department of Medicinal Chemistry, Amgen Inc., One Kendall Square, Building 1000, Cambridge, MA 02139, USA*
[b]*Department of Molecular Pharmacology, Amgen Inc., One Kendall Square, Building 1000, Cambridge, MA 02139, USA*
[c]*Department of Molecular Structure, Amgen Inc., One Kendall Square, Building 1000, Cambridge, MA 02139, USA*
[d]*Department of Oncology Research, Amgen Inc., One Amgen Center Drive, Thousand Oaks, CA 91320, USA*
[e]*Department of Pharmacokinetics & Drug Metabolism, Amgen Inc., One Amgen Center Drive, Thousand Oaks, CA 91320, USA*

Received 18 December 2006; revised 16 February 2007; accepted 21 February 2007
Available online 25 February 2007

Abstract—A novel class of selective Tie-2 inhibitors was derived from a multi-kinase inhibitor **1**. By reversing the amide connectivity and incorporating aminotriazine or aminopyridine hinge-binding moieties, excellent Tie-2 potency and KDR selectivity could be achieved with 3-substituted terminal aryl rings. X-ray co-crystal structure analysis aided inhibitor design. This series was evaluated on the basis of potency, selectivity, and rat pharmacokinetic parameters.

Inhibition of angiogenesis,[1] the formation of new capillaries from preexisting blood vessels, is a promising and clinically proven approach for limiting tumor growth and survival.[2] Angiogenesis is believed to be necessary for solid tumors to grow larger than 1–2 mm diameter, the point at which vasculature is required to supply oxygen and nutrients, and remove waste.[2,3] Disrupting the vascular endothelial growth factor (VEGF)/KDR (VEGFR-2) signaling cascade is a well-validated approach for inhibiting tumor growth as demonstrated by the FDA-approved anti-VEGF molecule, bevacizumab (Avastin™),[4] and small molecule kinase inhibitors, sunitinib (Sutent™)[5] and sorafenib (Nexavar™).[6] In contrast to the well-studied VEGF/KDR axis, the role of the competing interaction of angiopoietins (Ang-1 and Ang-2) with the Tie-2 receptor (tyrosine kinase with immunoglobulin and epidermal growth factor homology domains-**2**) in angiogenesis is less well understood.[7] The receptor tyrosine kinase Tie-2 is primarily expressed in the vascular endothelium and is involved in vessel branching, sprouting, remodeling, maturation, and stability.[7] Angiopoietin-1 binds to Tie-2 and stimulates tyrosine phosphorylation and signal transduction, resulting in blood vessel formation and/or maintenance.[8] The role of Angiopoietin-2 is controversial and has been shown to act as both an agonist and an antagonist of Tie-2 signaling.[7] The outcome of the Ang-2/Tie-2 interaction on vasculature depends on the presence/absence of VEGF and other proangiogenic factors.[7,9]

In order to evaluate the effect of Tie-2 kinase inhibitors on angiogenesis and tumor growth, we sought to develop small molecule inhibitors with high selectivity against kinases involved in angiogenesis, for example KDR. Previous work revealed pyridinyl pyrimidine **1** to be a potent, dual Tie-2/KDR inhibitor that served as a launching point for SAR studies (Fig. 1).[10] Herein, we describe an isomeric 'reversed-amide' series (e.g., **2**, where the amide linkage is reversed compared to **1**) that possesses good in vitro potency, selectivity, and unique

Keywords: Tie-2 kinase; Oncology; Small molecule kinase inhibitors; Triazine; KDR.
* Corresponding author. Tel.: +1 617 444 5090; fax: +1 617 621 3908; e-mail: bhodous@amgen.com

0960-894X/$ - see front matter © 2007 Elsevier Ltd. All rights reserved.
doi:10.1016/j.bmcl.2007.02.067

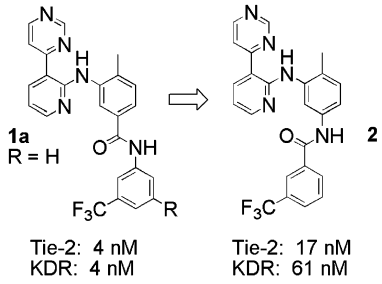

Figure 1. The potent, non-selective pyridinyl pyrimidine **1a** modified by reversing the amide orientation to arrive at **2**. **1b**, R = $-(CH_2)_3N(CH_3)_2$; Tie-2 = 1 nM, KDR = 2 nM.

SAR, but sub-optimal pharmacokinetic properties. X-ray co-crystallographic studies aided the SAR investigations.

All of the 'reversed-amide' analogs were synthesized in the manner outlined for **5** in Scheme 1. 2-*N*-Methylaminotriazine **3** can be synthesized on multi-gram scale as previously described.[10] This building block was reacted with 5-amino-2-methylphenol under basic conditions to displace the activated chloride and form penultimate biaryl ether intermediate **4**. Biaryl anilines (e.g., **2**) were not pursued due to poor physical properties (mp of **2** = 192 °C vs mp of **5** = 95 °C).[10] HATU-mediated coupling of the substituted benzoic acid to **4** afforded final compound **5** in 40% yield over two steps. 2-*N*-Methylaminopyrimidine (**9**) and pyridine (**11**, **15**, **16**, **20**) derivatives were synthesized in an analogous fashion.[10]

X-ray co-crystal structures of an amide **1b** (Tie-2 IC_{50} = 1 nM, KDR IC_{50} = 2 nM; similar selectivity profile to **1a**) and 'reversed-amide' **2** bound to the ATP-site of the Tie-2 kinase were solved (Fig. 2).[11] In each ligand, the pyrimidine ring makes identical key hydrogen bonds to the backbone NH of the linker residue, Ala905 (**1b** = 2.85 Å; **2** = 2.88 Å). This interaction situates the pyridine rings in alignment, and within edge-to-face π-stacking distance of Phe983 (~3.5 Å) of the DFG-motif (first three residues of the activation loop). The central and terminal aryl rings overlay with only slight differences in orientation, placing the CF_3-groups in essentially the same space in the extended hydrophobic pocket (EHP) in each series. Both amide arrangements engage in strong hydrogen bonds with Asp982 of the

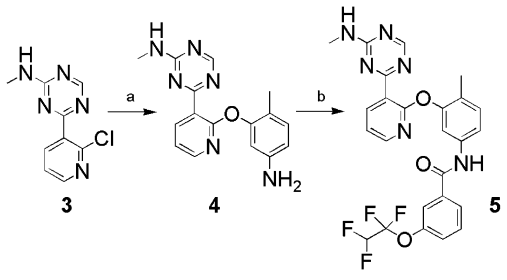

Scheme 1. Reagents and conditions: (a) 5-amino-2-methylphenol, Cs_2CO_3, DMSO, 130 °C, 62%; (b) 3-(1,1,2,2-tetrafluoroethoxy)benzoic acid, HATU, *i*-Pr_2NEt, $CHCl_3$, rt, 64%.

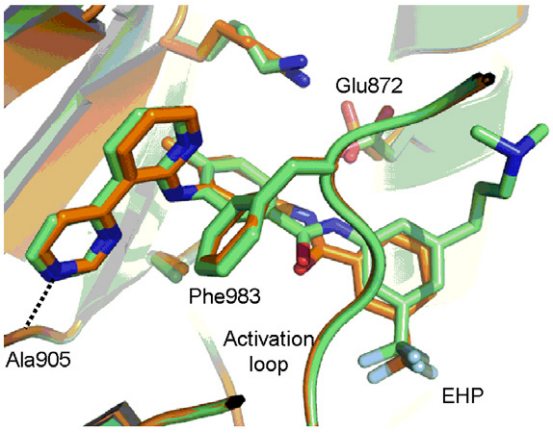

Figure 2. X-ray co-crystal structures of amide **1b** (green) and reversed-amide **2** (brown) bound to the ATP binding site of Tie-2. (Oxygen atoms (red), nitrogen atoms (blue), and fluorine atoms (light blue).)

DFG-motif and Glu872 of the αC-helix: **1b**, H-bonds = 2.92 and 2.91 Å; **2**, H-bonds = 3.04 and 2.73 Å.

Realizing the similarities in binding mode between **1b** and **2**, we initiated SAR studies with two modifications that were previously determined to be optimal: (1) *N*-methylamino-substituted hinge-binding heterocycles provided improved potency versus hydrogen substitution; (2) the biaryl ether series provided improved physical properties versus biaryl anilines (e.g., **9**–**11**, Table 1).[10] Although a potent Tie-2 inhibitor, reversed amide **9**, showed no improvement in selectivity over KDR versus the corresponding amide **6**. However, by changing the pyrimidine (**9**) to a triazine (**10**) or pyridine (**11**) hinge-binding moiety, selectivity over KDR was dramatically improved for the reversed amide without

Table 1. Comparison of enzyme potency (IC_{50}, nM) for amides and reversed-amides

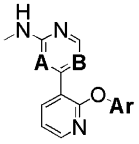

Compound	Ar	A	B	Enzyme (nM)	
				Tie-2	KDR
6	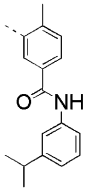	N	CH	13	38
7		N	N	1	20
8		CH	CH	3	5
9	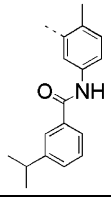	N	CH	2	2
10		N	N	1	117
11		CH	CH	1	18

Table 2. Tie-2 and KDR potency (IC_{50}, nM) and rat in vivo clearance (mL/h/kg) for central ring variations of triazines and pyridines

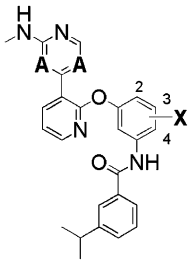

Compound	A	X	Enzyme (nM)		Cellular (nM)	Rat iv CL (mL/h/kg)
			Tie-2	KDR	Tie-2	
10	N	2-Me	1	117	5	3942
12	N	H	6	456	85	4421
13	N	2-F	4	128	—	1104
14	N	3-CF_3	55	25,000	—	—
11	CH	2-Me	1	18	11	3260
15	CH	H	4	18	—	—
16	CH	4-Cl	6	9	—	—

compromising potency for Tie-2 enzyme (**7** vs **10** and **8** vs **11**).

Encouraged by the low nanomolar potency and 100-fold selectivity of triazine **10**, we explored the SAR of the central aryl ring (Table 2). Replacement of the 2-methyl group with a hydrogen resulted in a significant loss in cellular potency (**10** vs **12**; Tie-2 autophosphorylation measured in EA.hy 926 cells). We determined that poor pharmacokinetic properties were the most significant issues with this reversed-amide series. Rat clearances equal to rat liver blood flow were observed for **10**, **11**, and **12**. Interestingly, a 2-fluoro derivative (**13**) led to a much reduced rat iv clearance (CL = 1104 mL/h/kg); however, this was accompanied by an undesirable half-life of 0.8 h (mean-residence time = 0.5 h). Other electron-withdrawing groups such as 3-CF_3 (**14**) resulted in sub-optimal enzyme inhibition; and 4-chloro lacked selectivity (**16**). In general, triazines provided superior selectivity over KDR and comparable potency on Tie-2 relative to pyridines (e.g., **10** vs **11** and **12** vs **15**).

In our SAR studies of the terminal aryl ring, we set out to reduce the rat in vivo clearance while maintaining potency and selectivity. Reducing the bulk of the hydrophobic substituent from isopropyl (**10**) to CF_3 (**17**) resulted in a decrease in potency and selectivity (Table 3). The 3-OCF_3 (**18**) and 3-pyrrolyl (**19**) groups imparted very good Tie-2 potency in the cellular autophosphorylation assay (IC_{50} = 15 and 23 nM, respectively), and impressive cellular selectivity over KDR (>1000-fold for **19**), but these compounds were rapidly cleared in rats. The highly fluorinated derivative **5**, did lead to a moderate clearance (CL = 889 mL/h/kg) compound that also maintained high potency and selectivity. The corresponding pyridine derivative **20** led to a high clearance molecule, although it was very potent in the Tie-2 cellular assay (IC_{50} = 13 nM).

Table 3. Tie-2 and KDR potency (IC_{50}, nM) and rat in vivo clearance (mL/h/kg) for terminal ring variation of triazines and pyridines

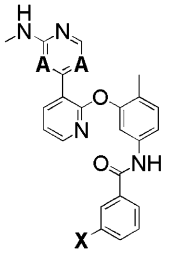

Compound	A	X	Enzyme (nM)		Cellular (nM)		Rat iv CL (mL/h/kg)
			Tie-2	KDR	Tie-2	KDR	
17	N	–CF_3	20	309	—	—	—
18	N	–OCF_3	8	442	15	540	4980
19	N		17	1126	23	25,000	3825
5	N		16	1002	33	4300	889
20	CH		9	233	13	943	3640

Table 4. Kinase selectivity summary for **5** (IC_{50}, nM)

Enzyme inhibition			
Tie-2	16	cKit	17,800
p38α	47	cMet	25,000
Lck	146	EGFR	25,000
KDR	1002	IGFR-1	25,000
Jak2	1746	Zap70	25,000
Src	2195	BTK	25,000
FGFR	5360	JNK3	40,000

Table 5. Rat pharmacokinetic properties for **5**[a]

iv administration[b]		po administration[c]	
$t_{1/2}$	1.7 h	%F	4
CL	889 mL/h/kg	C_{max}	119 ng/mL
V_{ss}	1311 mL/kg	AUC_{0-inf}	509 ng h/mL

[a] $N = 3$ animals/group.
[b] Dosed intravenously at 2 mg/kg in DMSO to male Sprague–Dawley rats.
[c] Dosed orally at 10 mg/kg as a suspension in 2% HPMC/1% Tween 80/97% water (pH 2.2) to male Sprague–Dawley rats.

Based on Tie-2 cellular potency ($IC_{50} = 33$ nM), excellent selectivity over KDR (63-fold enzyme selectivity; 130-fold cellular selectivity), and promising pharmacokinetics, we chose **5** for further profiling. The selectivity profile was explored across a range of tyrosine and serine/threonine kinases (Table 4). The phosphorylation of serine/threonine kinase p38α ($IC_{50} = 47$ nM) and non-receptor tyrosine kinase Lck ($IC_{50} = 146$ nM) was inhibited most strongly. The p38α activity was examined in a THP-1/TNFα cellular assay,[12] resulting in an $IC_{50} = 194$ nM. All of the other tested kinases in the selectivity panel returned potency values of greater than one micromolar.

The rat pharmacokinetic parameters for **5** are summarized in Table 5. Data collected from intravenous dosing were a moderate clearance and volume of distribution, leading to a half-life of 1.7 h (mean-residence time = 1.5 h). Unfortunately, when **5** was dosed po at 10 mg/kg an oral bioavailability of 4% was achieved. One possible factor contributing to the low %F could be the inadequate solubility at pH values of 2 and 7.1 (solubility: 0.01 N HCl = 0.021 mg/mL; phosphate-buffered solution = 0.003 mg/mL).[13]

In conclusion, a number of highly potent inhibitors of Tie-2 cellular autophosphorylation were discovered in this reversed-amide series. Impressive levels of selectivity over KDR and a panel of other kinases were achieved within the triazine series. Compound **5** possessed the best combination of potency, selectivity, and rat pharmacokinetics; however, further improvement is required to enhance oral bioavailability. Modifications to this promising scaffold that address these parameters will be reported in subsequent publications.

Supplementary data

Supplementary data associated with this article can be found, in the online version, at doi:10.1016/j.bmcl.2007.02.067.

References and notes

1. Risau, W. *Nature* **1997**, *386*, 671.
2. (a) Folkman, J. *Ann. Surg.* **1972**, *175*, 409; (b) Folkman, J. *N. Engl. J. Med.* **1971**, *285*, 1182.
3. (a) Holmgren, L.; O'Reilly, M. S.; Folkman, J. *Nat. Med.* **1995**, *1*, 149; (b) Folkman, J. *J. Nat. Cancer Inst.* **1990**, *82*, 4.
4. Mulcahy, M. F.; Benson, A. B., III *Expert Opin. Biol. Ther.* **2005**, *5*, 997.
5. Sun, L.; Liang, C.; Shirazian, S.; Zhou, Y.; Miller, T.; Cui, J.; Fukuda, J. Y.; Chu, J.-Y.; Nematalla, A.; Wang, X.; Chen, H.; Sistla, A.; Luu, T. C.; Tang, F.; Wei, J.; Tang, C. *J. Med. Chem.* **2003**, *46*, 1116.
6. Strumberg, D.; Richly, H.; Hilger, R. A.; Schleucher, N.; Korfee, S.; Tewes, M.; Faghih, M.; Brendel, E.; Voliotis, D.; Haase, C. G.; Schwartz, B.; Awada, A.; Voigtmann, R.; Scheulen, M. E.; Seeber, S. *J. Clin. Onc.* **2005**, *5*, 965.
7. Yu, Q. *Future Med.* **2005**, *1*, 475.
8. Cho, C.-H.; Kammerer, R. A.; Lee, H. J.; Steinmetz, M. O.; Ryu, Y. S.; Lee, S. H.; Yasunaga, K.; Kim, K.-T.; Kim, I.; Choi, H.-H.; Kim, W.; Kim, S. H.; Park, S. K.; Lee, G. M.; Koh, G. Y. *Proc. Natl. Acad. Sci. U.S.A.* **2004**, *101*, 5547.
9. (a) Scharpfenecker, M.; Fielder, U.; Reiss, Y.; Augustin, H. G. *J. Cell Sci.* **2005**, *118*, 771; (b) Lobov, I. B.; Brooks, P. C.; Lang, R. A. *Proc. Natl. Acad. Sci. U.S.A.* **2002**, *99*, 11205.
10. Synthetic procedures and conditions for HTRF and cellular assays are described in: Hodous, B. L.; Geuns-Meyer, S. D.; Hughes, P. E.; Albrecht, B. K.; Bellon, S.; Bready, J.; Caenepeel, S.; Cee, V. J.; Chaffee, S. C.; Coxon, A.; Emery, M.; Fretland, J.; Gallant, P.; Gu, Y.; Hoffman, D.; Johnson, R. E.; Kendall, R.; Kim, J. L.; Long, A. M.; Morrison, M.; Olivieri, P. R.; Patel, V. F.; Polverino, A.; Rose, P.; Tempest, P.; Wang, L.; Whittington, D. A.; Zhao, H. *J. Med. Chem.* **2007**, *50*, 611.
11. The PDB deposition code for **1b** is 2OO8 and for **2** is 2OSC.
12. Lin, T. H.; Metzger, A.; Diller, D. J.; Desai, M.; Henderson, I.; Ahmed, G.; Kimble, E. F.; Quadros, E.; Webb, M. L. *J. Pharmacol. Exp. Ther.* **2006**, *318*, 495.
13. Tan, H.; Semin, D.; Wacker, M.; Cheetham, J. *J. Assoc. Lab. Automat.* **2005**, 364.